Erosion and Re-deposition of Plasma-Facing material in Long Duration Discharges on TRIAM-1M

Sakamoto, Mizuki
Research Institute for Applied Mechanics, Kyushu University

Ogawa, Masanori
Interdisciplinary Graduate School of Engineering Sciences, Kyushu University

Higashizono, Yuta
Research Institute for Applied Mechanics, Kyushu University

Zushi, Hideki
Research Institute for Applied Mechanics, Kyushu University

他

https://doi.org/10.15017/27047

出版情報：九州大学応用力学研究所所報. 136, pp.19-22, 2009-03. Research Institute for Applied Mechanics, Kyushu University
バージョン：
権利関係：

Erosion and Re-deposition of Plasma-Facing material in Long Duration Discharges on TRIAM-1M

Mizuki SAKAMOTO*[1], Masanori OGAWA*[2], Yuta HIGASHIZONO*[1], Hideki ZUSHI*[1], Kohnosuke SATO*[1], Kazuo NAKAMURA*[1], Kazuaki HANADA*[1], Hiroshi IDEI*[1], Makoto HASEGAWA*[1], Shoji KAWASAKI*[1], Hisatoshi NAKASHIMA*[1], Aki HIGASHIJIMA*[1]

E-mail of corresponding author: *sakamoto@triam.kyushu-u.ac.jp*

(Received January 30, 2009)

Abstract

Properties of erosion and re-deposition of plasma-facing material in TRIAM-1M has been studied. The thickness of the re-deposited layer was estimated using the optical reflectivity on the sapphire window. Oxygen impurities should dominate the erosion and deposition properties of the plasma-facing wall as well as the hydrogen retention property of the co-deposited layer.

Key words : *Plasma-Wall Interaction, Erosion, Re-deposition*

1. Introduction

Plasma-wall interaction (PWI) issues are strongly related to plasma performance and stable operation, and are especially critical for a steady state operation (SSO) of fusion plasma [1-3].

In TRIAM-1M, which had SSO capability, plasma-wall interaction experiments have been carried out extensively from microscopic and macroscopic viewpoints [4-16]. The co-deposition of hydrogen with the plasma-facing material of molybdenum is considered to be dominant for the continuous wall pumping in TRIAM-1M. In this paper, erosion and re-deposition of plasma-facing material is presented.

2. Experimental Setup

TRIAM-1M is a superconducting tokamak. Sixteen superconducting toroidal field coils composed of Nb_3Sn were installed. The toroidal magnetic field was up to 8 T and in the steady state. The poloidal field coils of Cu were mounted on a vacuum vessel with a D-shaped cross-section, a horizontal length of 0.26 m, and the vertical length of 0.38 m. The major radius of the center of the vacuum vessel was 0.84 m. The entire machine was installed inside a bell-shaped vacuum vessel (i.e. a bell-jar) for thermal insulation. Extension ports connected the plasma vacuum vessel and the bell-jar.

The plasma-facing components were made of high Z materials: three fixed poloidal limiters (PLs) and divertor plates were made of molybdenum, and the vacuum vessel (i.e. main chamber) was stainless steel. A movable limiter (ML) with a front edge made of molybdenum was installed in the same section as the fixed poloidal limiter and the pumping port. The ML was thermally insulated from the main chamber, and had a good cooling capability. A low Z material coating was not applied. Wall conditioning was performed just prior to the experimental campaign. The extension ports were initially heated to 100 °C for ~2 days, and then electron cyclotron resonance discharge cleaning for ~2 days was carried out to clean the plasma-facing components [17,18]. To avoid a thermal load to the cryogenic system, the plasma vacuum vessel was not heated. The main chamber was evacuated using a turbo-molecular-pump with an effective pump speed of 550 l s^{-1}.

The plasma current was initiated by ohmic heating (τ~0.2s), and then sustained by a lower hybrid

*0 Research Institute for Applied Mechanics, Kyushu University
*1 Interdisciplinary Graduate School of Engineering Sciences, Kyushu University

current drive (LHCD) with a frequency of 2.45 GHz or 8.2 GHz. It should be noted that all the results reported herein were obtained from hydrogen discharges with a limiter configuration.

3. Experimental Results and Discussion

The co-deposition of hydrogen with molybdenum may play an important role on the continuous wall pumping in a long duration discharge in TRIAM-1M. In order to study the properties of erosion and re-deposition of plasma-facing materials, a real time, in situ measurement system for erosion and deposition has been developed in TRIAM-1M [19]. This system is based on light interference on a thin semi-transparent layer of re-deposited material on the substrate [20]. A 4 mm thick sapphire window was used as a substrate, which was also used for Thomson scattering measurement. The window was about 75 mm from the last closed flux surface of the plasma that was at the center of the poloidal limiter. A fiber optic bundle, which was composed of 450 optic fibers with a 100 μm diameter, was attached to the air side of the window. The optic fibers were mixed statistically. The fiber optic bundle was pushed on the window surface by spring action to avoid a gap between the bundle and window due to vibrations during the plasma production. Half of the optic fibers were used to illuminate the substrate with laser light (λ ~635 nm), while the other half guided the reflected light back to a photodiode. In order to avoid plasma light, an interference filter was mounted in front of the photodiode. The intensity of the laser light was monitored by the other photodiode.

Figure 1(a) shows the deposition pattern on a sapphire window after the last experimental campaign in 2005. The experimental period was 1.5 month. The cross in Fig.1(a) indicates the measurement position of erosion and deposition. The thickest part of the deposited layer (> 20 nm) was located at the lower left, and the deposition pattern was asymmetric relative to the mid-plane of the vacuum vessel. The likely molybdenum source for the deposition on the sapphire window was the divertor plate, which was located at the bottom of the vacuum vessel. The divertor plate was sputtered by charge exchange neutral hydrogen, and some of the sputtered molybdenum atoms can reach the sapphire window. A previous experiment has reported that all the deposits formed on a specimen placed in a vacuum vessel for the duration of an experimental campaign were molybdenum, and the major elemental components (i.e. iron, chromium, and nickel) of the vacuum vessel were not detected [4]. Figure 1(b) shows the angular distribution of the

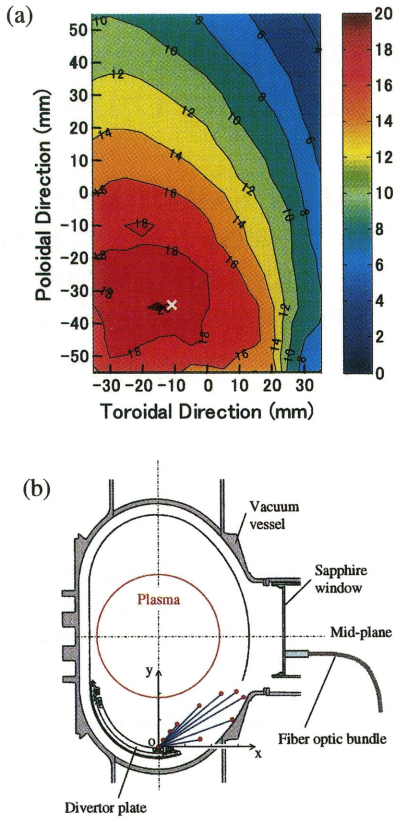

Fig.1 (a) Mo deposition pattern on the sapphire window after the last experimental campaign in 2005. (b) Diagram of the angular distribution of sputtered Mo atoms from the divertor plate superimposed on the cross-section of the vacuum vessel.

sputtered molybdenum atoms from the divertor plate. The length from the origin corresponds to the number of molybdenum atoms capable of reaching the wall through the SOL plasma. Because the molybdenum atoms, which reach the upper part of the window, must pass through a higher density and higher temperature region and its pass length becomes longer, fewer molybdenum atoms can reach the upper part of the window. This may be the reason for the up-down asymmetry of the deposition pattern. As for the toroidal direction, the deposition pattern was weighted toward the ion drift side, suggesting anisotropic sputtering in the toroidal direction.

The net erosion and deposition rate on the window depended on the discharge conditions, and ranged between -2×10^{-3} nm s^{-1} to 2×10^{-3} nm s^{-1} for long duration discharges ($0.1 \times 10^{19} m^{-3} \leq \bar{n}_e \leq 1 \times 10^{19} m^{-3}$). The positive and negative signs indicate deposition and erosion, respectively. Figure 2 shows a typical result in a high power and high density

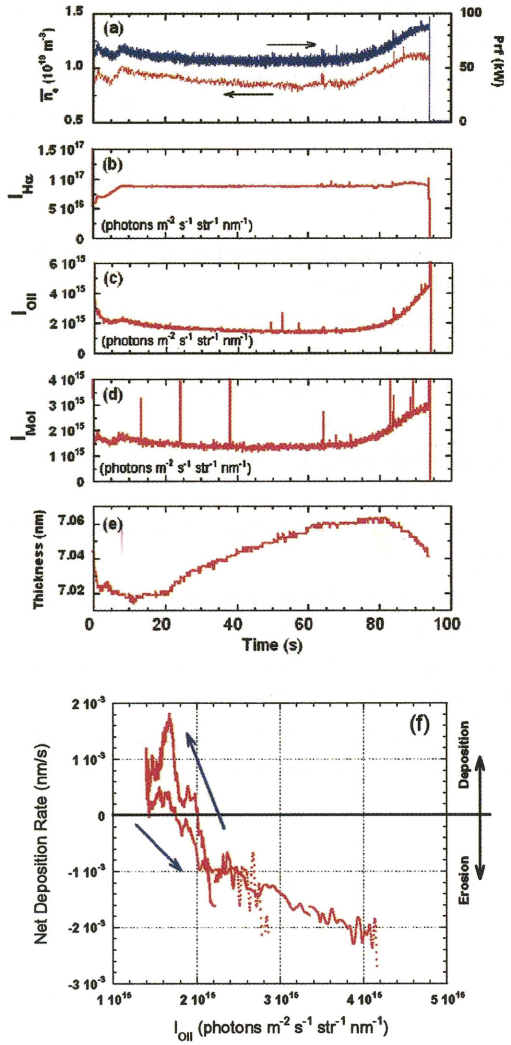

Fig.2 Time evolution of (a) the line average electron density, (b) H_α line intensity, (c) OII line intensity, (d) MoI line intensity, (e) thickness of deposited layer, and (f) deposition rate as a function of OII line intensity.

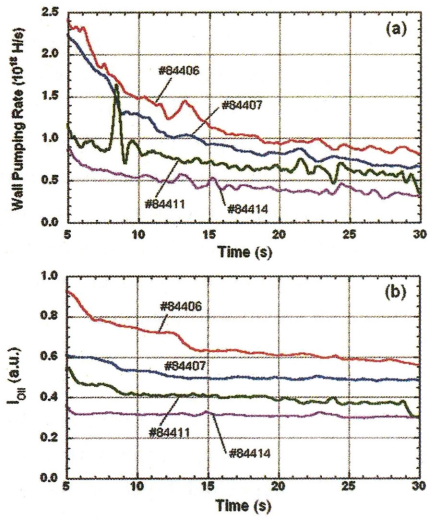

Fig.3 Time evolution of (a) wall pumping rate and (b) OII intensity in the initial discharge phase.

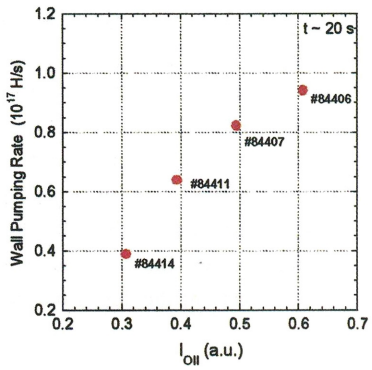

Fig.4 Wall pumping rate at t~20 s as a function of OII line intensity.

discharge in 8.2GHz LHCD. In the latter phase of the discharge, the plasma density increased due to enhanced PWI, although the gas feed was terminated. The net RF power simultaneously increased because the RF coupling with plasma improved due to the increase in the SOL density. In addition, the reflected power decreased. The OII line intensity and MoI line intensity also increased during the latter phase, but the H_α line intensity remained constant. It was found that the thickness of the deposited layer decreased in earlier and latter phases of the discharge (i.e., erosion phase), but increased in the middle phase of the discharge (i.e., deposition phase), as shown in Fig.2(e). Figure 2(f) shows the deposition rate as a function of OII line intensity, which is considered to be related to oxygen flux. It seems that oxygen impurities affected the erosion property, and a critical value exists for the oxygen flux during the transition from deposition to erosion, and vice versa. In a low density discharge (i.e., low oxygen amount), the deposition rate seems to depend on the ratio of molybdenum flux Γ_{Mo} to hydrogen flux Γ_H, i.e. Γ_{Mo}/Γ_H [19].

A previous study on hydrogen recycling [6] has clearly demonstrated that in the initial phase of a long duration discharge, the hydrogen recycling coefficient increases with two different time constants: a few seconds and ~30 s. In this period, the recycling coefficient changed significantly. Figure 3(a) shows the time evolution of the wall pumping rate in the initial phase of a long duration discharge. The decreased wall pumping rate means that the recycling coefficient increased. It was found that the wall pumping rate decreased shot-by-shot. The OII line intensity implies

the same tendency as the wall pumping rate shown in Fig.3(b). Figure 4 shows the wall pumping rate as a function of the OII line intensity. The global wall pumping rate seems to correlate with the oxygen behavior. Oxygen impurities affected the physicochemical properties of the deposits, and then the capability of hydrogen retention of the deposits increased significantly. The result of Fig.4 may suggest the impact of co-deposition of hydrogen with oxygen and molybdenum on global wall pumping.

3. Conclusion

In TRIAM-1M, in situ and real time measurement system for erosion and re-deposition was developed. The thickness of the deposited layer on the sapphire window was estimated from optical reflectivity of the window. The source of re-deposited material was the divertor plate made of molybdenum. The net erosion and re-deposition rate on the window ranged between -2×10^{-3} nm s^{-1} to 2×10^{-3} nm s^{-1} for long duration discharges (0.1×10^{19} $m^{-3} \leq \bar{n}_e \leq 1 \times 10^{19}$ m^{-3}). During high density discharge ($\bar{n}_e \sim 1 \times 10^{19}$ m^{-3}), there were both phases of erosion and re-deposition. It seemed that oxygen impurities affected the erosion property, and a critical value existed for the oxygen flux during the transition from erosion to re-deposition, and vice versa. Oxygen impurities should dominate the erosion and re-deposition on the wall as well as the hydrogen retention property of the deposited layer.

Acknowledgements

This work has been partially performed under the framework of joint-use research in RIAM Kyushu University and the bi-directional collaboration organized by NIFS. This work is partially supported by a Grant-in-Aid for Science Research from the Ministry of Education, Culture, Sports, Science and Technology.

References

[1] M. Shimada, A.E. Costley et al., J. Nucl. Mater., **337-339** (2005) 808.
[2] V. Philipps, Physica Scripta, **T123** (2006) 24.
[3] E. Tsitrone, J. Nucl. Mater., **363-365** (2007) 12.
[4] T. Hirai, T. Fujiwara et al., J. Nucl. Mater., **283-287** (2000) 1177.
[5] T. Hirai, T. Fujiwara et al., J. Nucl. Mater., **290-293** (2001) 94.
[6] M. Sakamoto, et al., Nucl. Fusion **42** (2002) 165.
[7] M. Sakamoto, H. Nakashima et al., J. Nucl. Mater. **313-316** (2003) 519.
[8] Y. Hirooka, M. Sakamoto, The TRIAM group, J. Nucl. Mater., **313-316** (2003) 588.
[9] M. Sakamoto, M. Yuno et al., Nucl. Fusion, **44** (2004) 693.
[10] H. Zushi et al., Nucl. Fusion, **45** (2005) S142.
[11] K. Hanada, T. Sugata et al., Fus. Eng. Design **81** (2006) 2257.
[12] M. Miyamoto, K. Tokunaga et al., J. Nucl. Mater., **313-316** (2003) 82.
[13] M. Miyamoto, M. Tokitani et al., J. Nucl. Mater., **337-339** (2005) 436.
[14] M. Tokitani, M. Miyamoto et al, J. Nucl. Mater., **367-370** (2007) 1487.
[15] M. Ogawa, M. Sakamoto et al., J. Nucl. Mater., **363-365** (2007) 1364.
[16] R. Bhattacharyay, H. Zushi et al., Nucl. Fusion, **47** (2007) 864.
[17] E. Jotaki and S. Itoh, Fusion Eng. Des., **36** (1997) 447.
[18] K. Hanada, E. Jotaki et al., Fusion Eng. Des., **54** (2001) 79.
[19] M. Sakamoto, M. Ogawa et al., J. Nucl. Mater., **363-365** (2007) 233.
[20] F. Weschenfelder, P. Wienhold and J. Winter, J. Nucl. Mater., **196-198** (1992) 1101.